Electronic Supplementary Material (ESI) for Journal of Materials Chemistry A. This journal is © The Royal Society of Chemistry 2021

Supporting Information

Surface Reconstruction of NiCoP for Enhanced Biomass Upgrading

Honglei Wang, Chong Li, Jintao An, Yuan Zhuang, and Shengyang Tao*

Department of Chemistry, School of Chemical Engineering, Dalian University of Technology, Dalian 116024, China.

Supplementary Figures and Tables

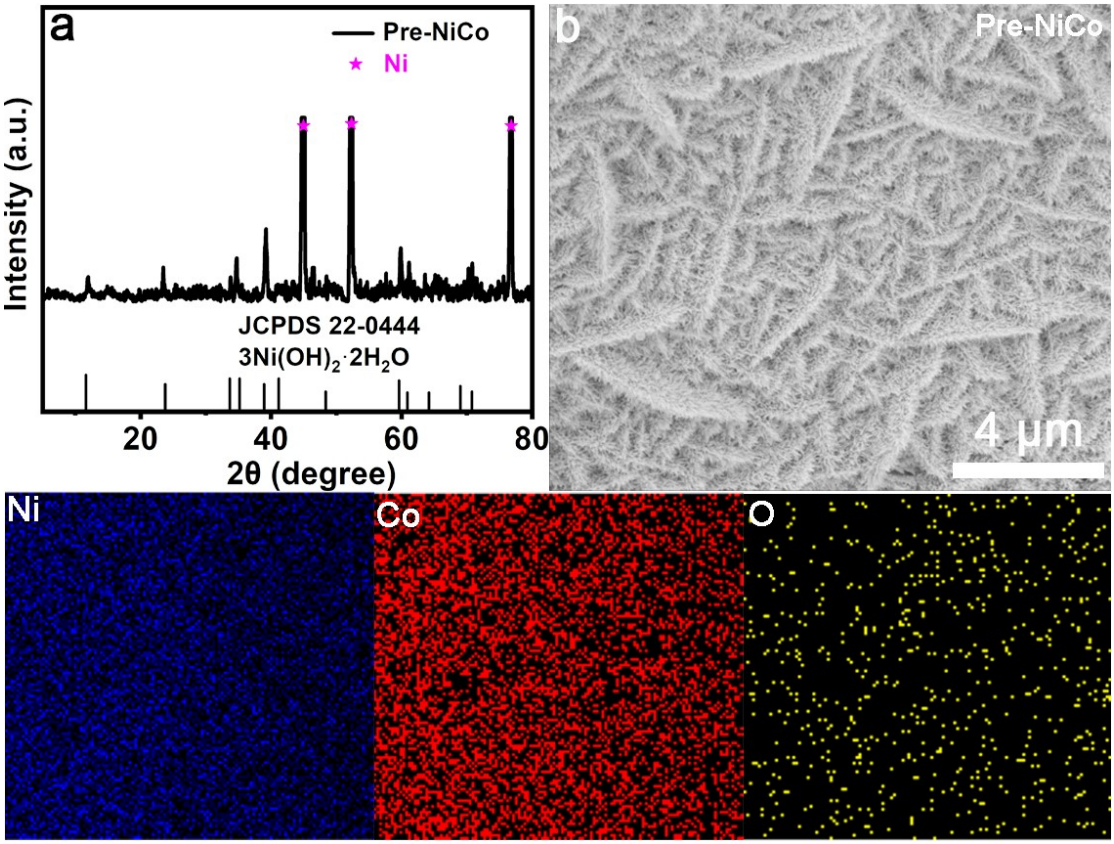

Fig. S1. (a) The XRD patterns of Pre-NiCo and (b) the SEM images and corresponding elements mapping for Pre-NiCo.

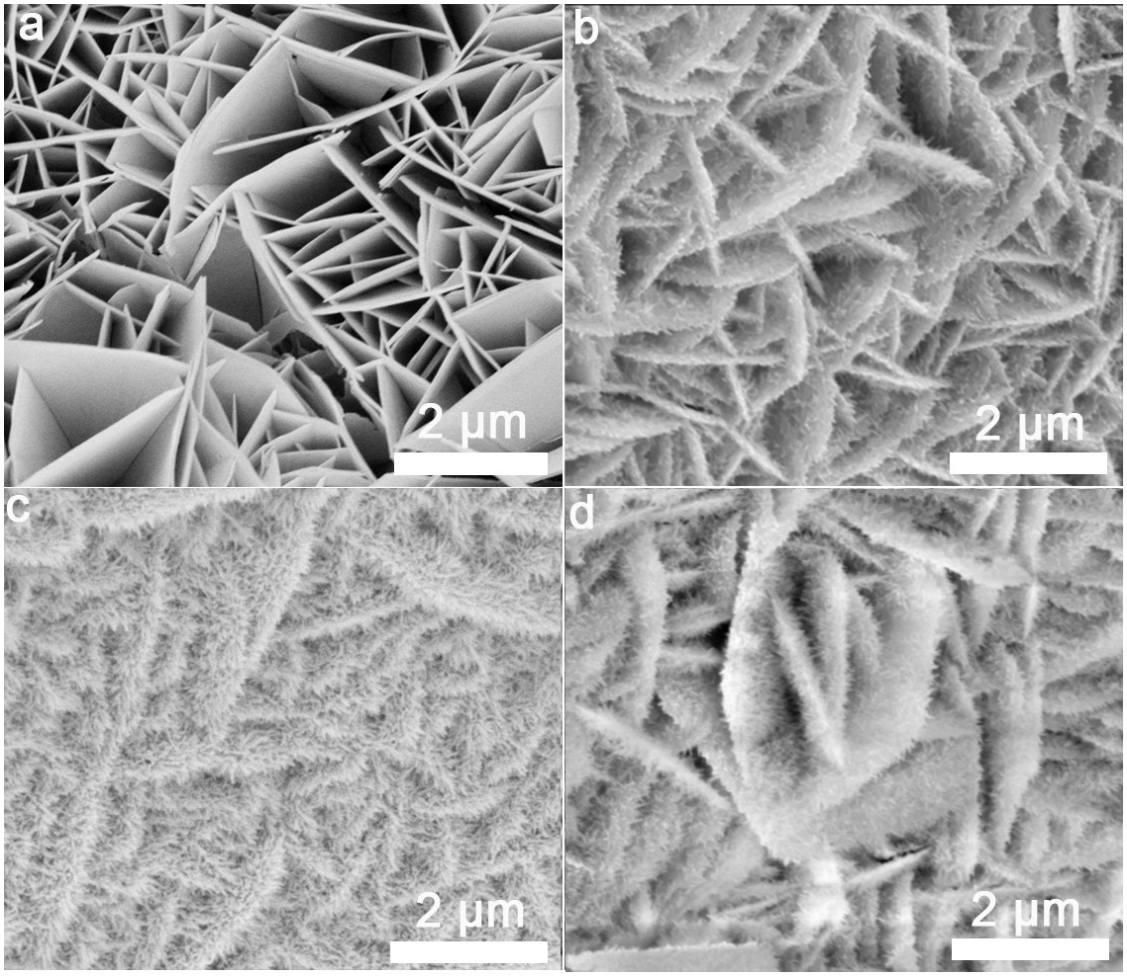

Fig. S2. Microscopy measurements of the Pre-NiCo at different reaction time with the same reaction temperature of 87 ˚C. SEM images of Pre-NiCo prepared at different reaction time (5 h (a), 10 h (b), 15 h (c), and 20 h (d)).

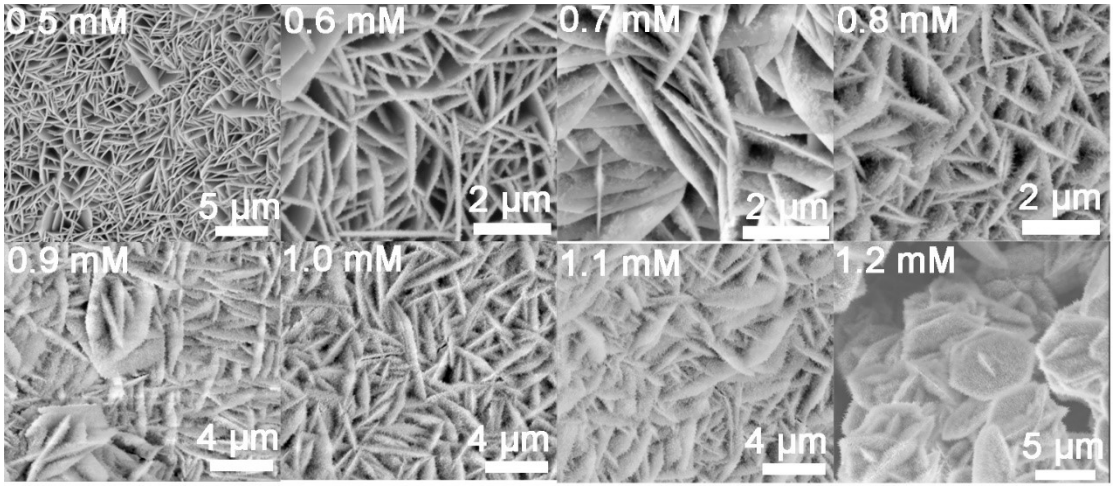

Fig. S3. SEM images of Pre-NiCo with different Co salts content under the same other conditions.

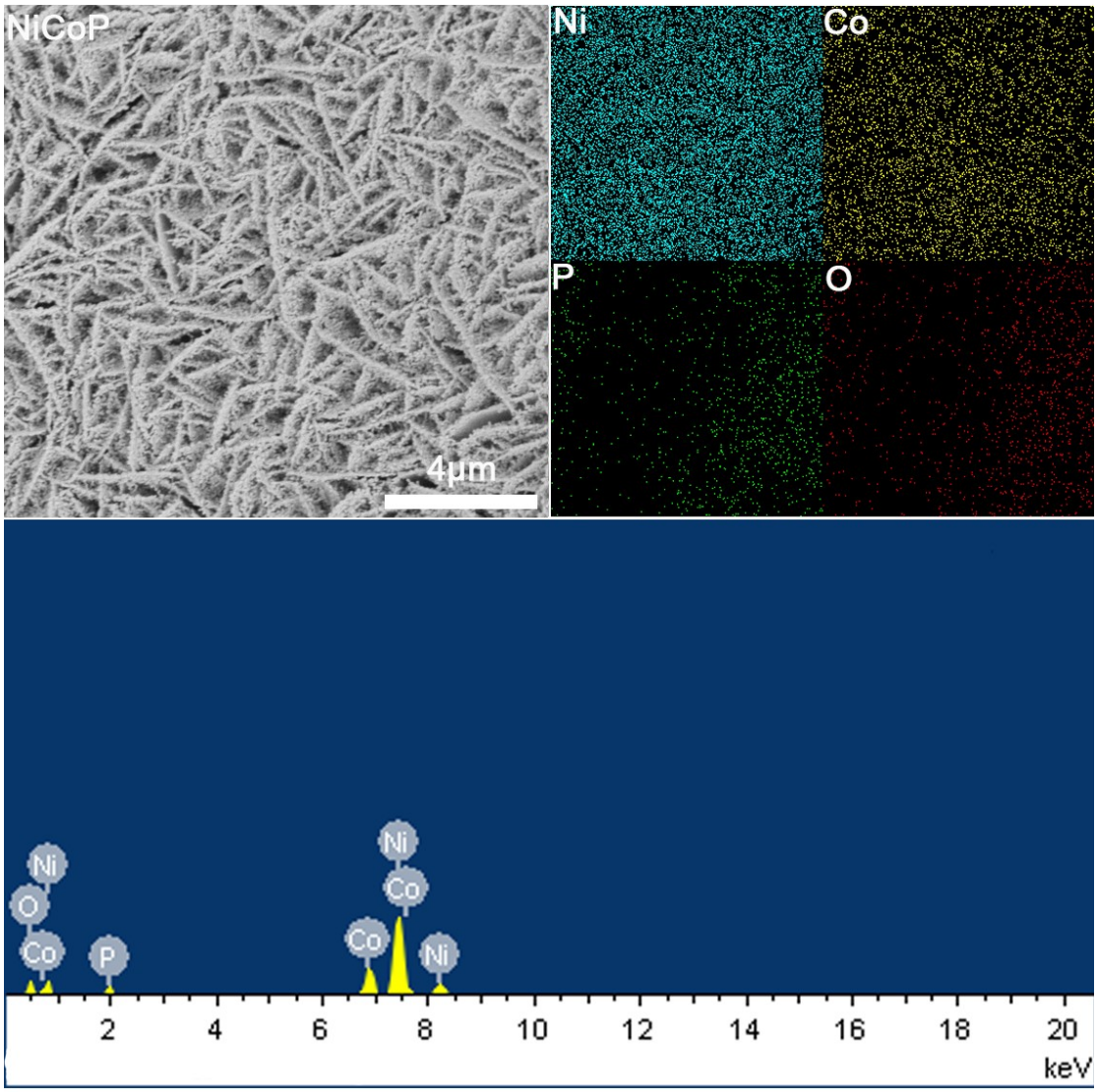

Fig. S4. The SEM images elements mapping and EDS of NiCoP.

Table S1. The mass percentage and atomic percentage of elements in NiCoP catalyst.

Elements	Mass ratio	Atomic
O	21.76	46.18
P	16.65	18.25
Co	14.87	8.57
Ni	46.71	27.01
Total	100	

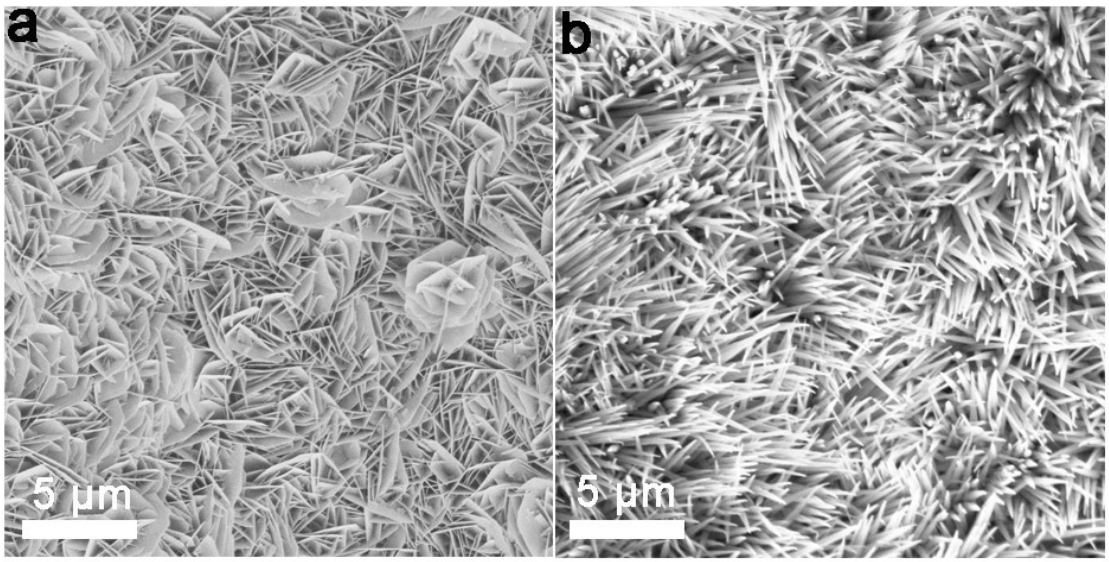

Fig. S5. The SEM images of Ni_2P (a) and (b) CoP.

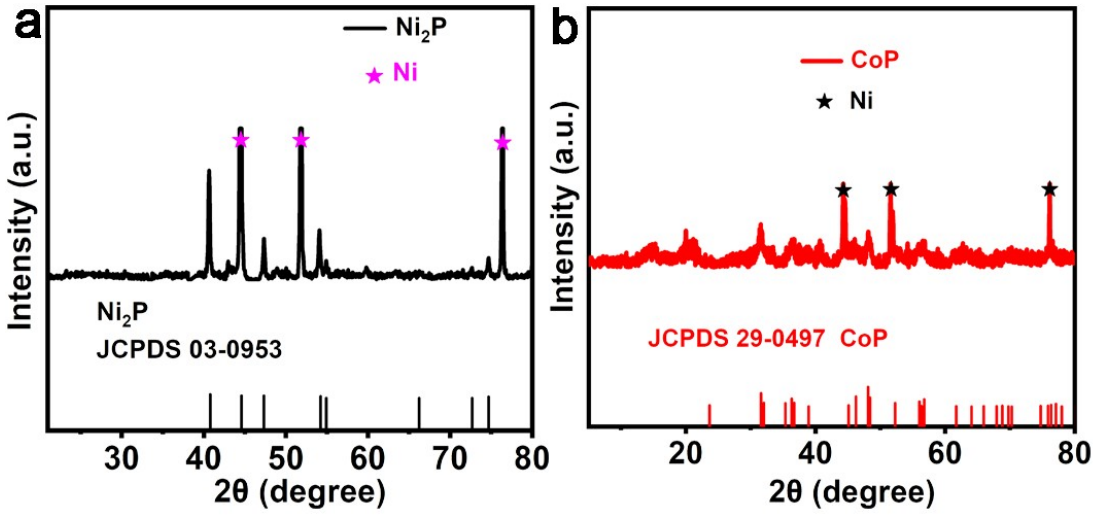

Fig. S6. The XRD patterns of Ni_2P (a) and (b) CoP.

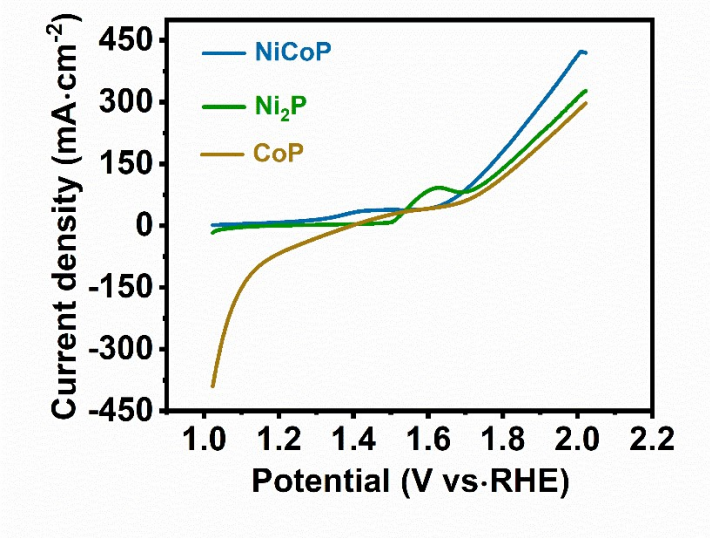

Fig. S7. The LSV curves of NiCoP, Ni_2P, and CoP at 1.0 M KOH.

Table S2. Comparison HMFOR performance of NiCoP with other electrocatalysts in 1.0 M KOH with 300 mM HMF.

Samples	Oxidation voltage (V vs RHE)	HMF Conversion (%)	FDCA Selectivity (%)	Faraday efficiency (%)	HMF concentration (mM)	Reference
NiOOH	1.47	99.8	95.8	96.0	5.0	1
MoO_2- FeP@C	1.45	99.4	98.6	97.8	10	2
NiSe@NiO_x/NF	1.35 (onset)	99.0	98.0	98.0	10	3
Ni_3N@C/NF	1.38	99.0	98.0	99.0	10	4
Co-P	1.44	~100	90.0	~90.0	50	5
$NiCo_2O_4$	1.50	90.4	90.8	87.5	5.0	6
VN/NiF	1.36	98	96	84	10	7
MnO_x	1.6	99.9	53.8	33.8	20	8
$CuCo_2O$	1.45	~100	93.7	94	50	9
CoNiFe LDH	1.55	95.5	84.9	~90.0	10	10
om-Co_3O_4/NF	1.457	~100	99.8	~100	10	11
$(PdAu)_7$	0.82	~	17.5	85.8	10	12
NiCoP	1.464	99.8	99.6	96.1	300	This work

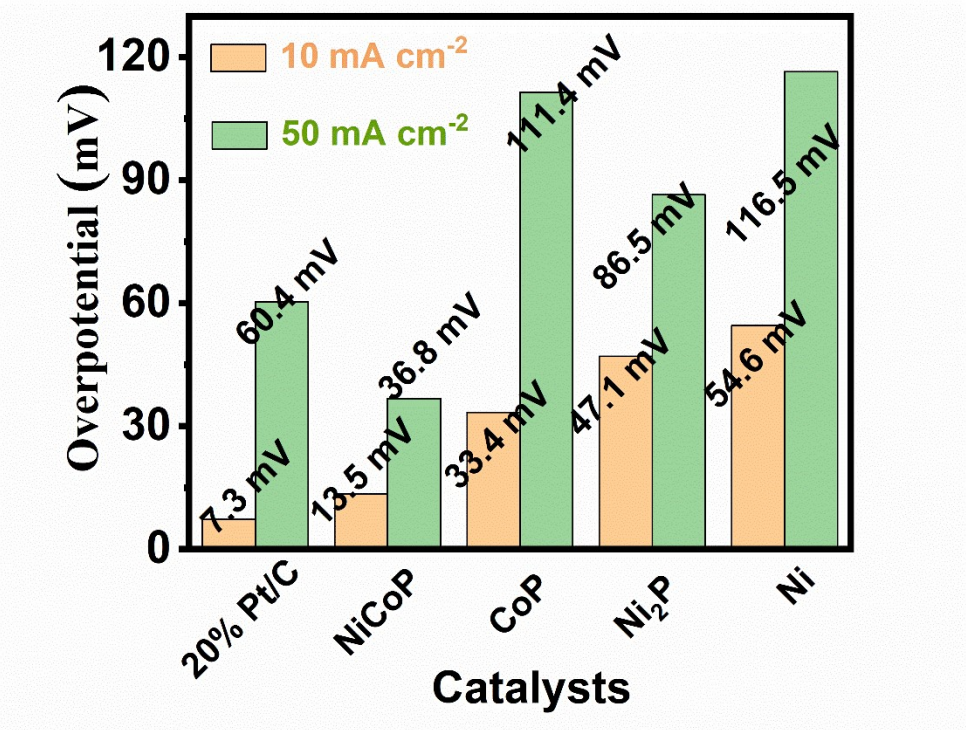

Fig. S8. The hydrogen evolution overpotential of 20% Pt/C, NiCoP, Ni_2P, CoP, and Ni with different current densities.

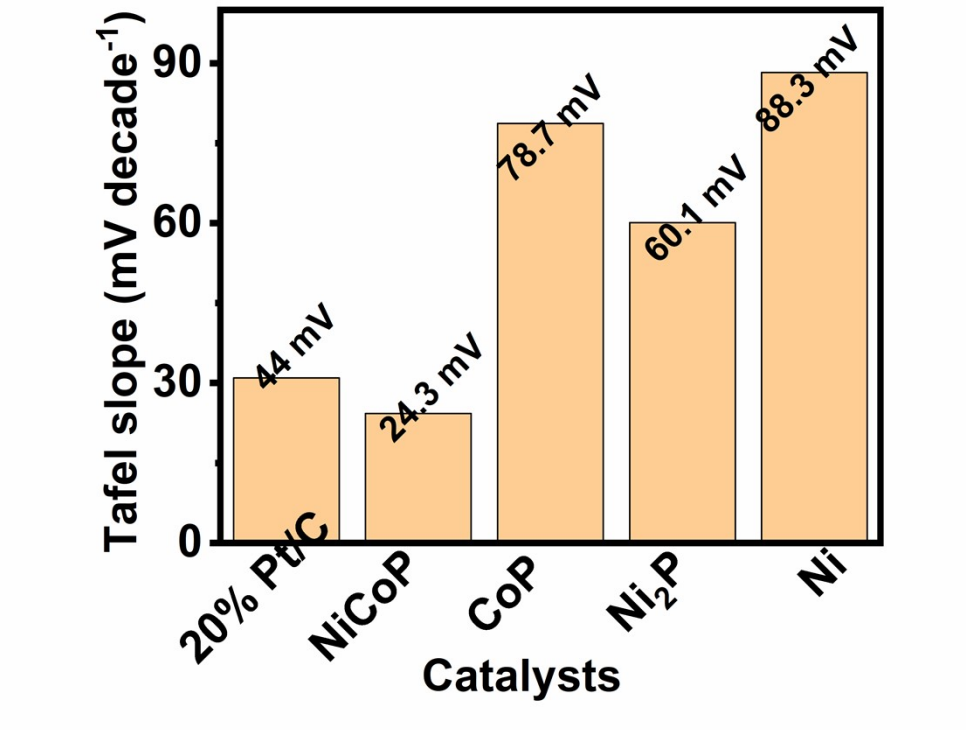

Fig. S9. The Tafel slope of 20% Pt/C, NiCoP, Ni_2P, CoP, and Ni.

Table S3. Comparison HER performance of NiCoP with other electrocatalysts.

Catalyst	Current density (j)	Overpotential at the corresponding (j)	Electrolye solution	Reference
NiCoP	10 mA/cm^2	13.5 mV	1.0 M KOH	This work
$RhSe_2$	10 mA/cm2	81.6 mV	1.0 M KOH	13
PS-MoNi@NF	10 mA/cm^2	30 mV	1.0 M KOH	14
Ni_3N-Co_3N PNAs/NF	10 mA/cm^2	43 mV	1.0 M KOH	15
Ni_4Mo	100 mA/cm^2	86 mV	1.0 M KOH	16
MoP/Mo_2N	10 mA/cm^2	89 mV	1.0 M KOH	17
NiP_2-650(c/m)	10 mA/cm^2	134 mV	1.0 M KOH	18
Cr−Ni	10 mA/cm^2	203 mV	1.0 M KOH	19
Ni_2P−Cu_3P	10 mA/cm^2	78 mV	1.0 M KOH	20
$PtNi_5$-0.3	10 mA/cm^2	26.8 mV	1.0 M KOH	21
CuAlNiMoFe	100 mA/cm^2	56 mV	1.0 M KOH	22
Co-N_4	10 mA/cm^2	66.7 mV	1.0 M KOH	23
Ru@WNO-C	10 mA/cm^2	24 mV	1.0 M KOH	24
MoS_2–MoP/NC,	10 mA/cm^2	35 mV	1.0 M KOH	25
PHA-Mo_2C	10 mA/cm^2	93 mV	1.0 M KOH	26
Ni_3N-V_2O_3-3-1	10 mA/cm^2	57 mV	1.0 M KOH	27
N-NiMoS	10 mA/cm^2	68 mV	1.0 M KOH	28
2DPC-Ru	10 mA/cm^2	24 mV	1.0 M KOH	29
Ni-$ReSe_2$	10 mA/cm^2	109 mV	1.0 M KOH	30

Table S4. The exchange current densities of the catalysts for HER.

Catalyst	Exchange current density in acid solution (mA cm^{-2})
20% Pt/C	6.25
NiCoP	2.82
CoP	2.69
Ni_2P	1.77
Ni	1.67

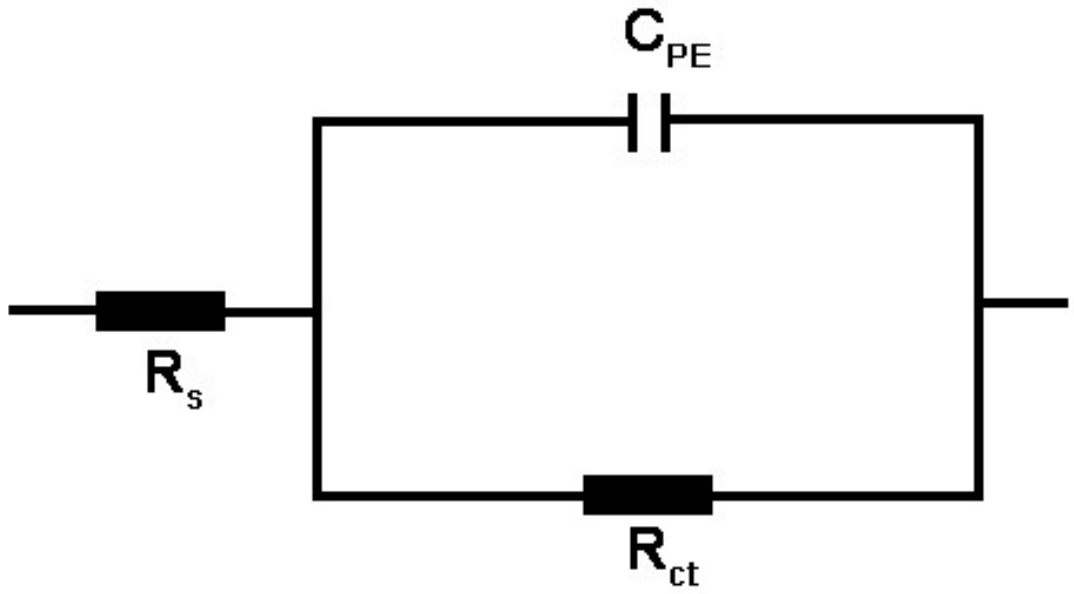

Fig. S10. The equivalent circuit of electrochemical impedance spectroscopy.

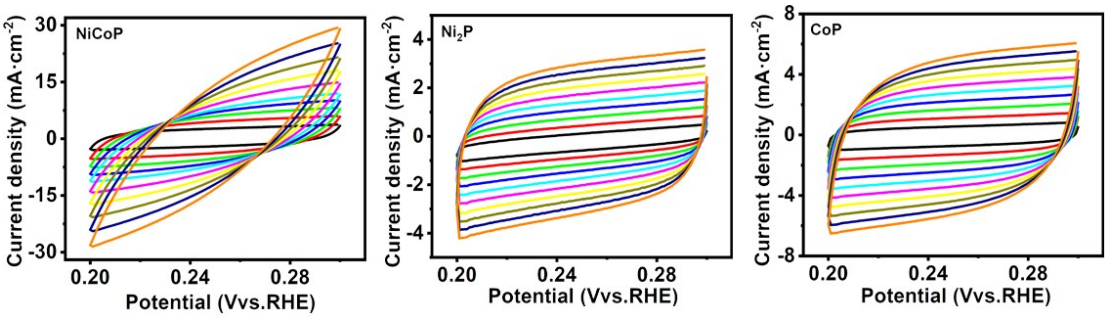

Fig. S11. The cyclic voltammetry curves for NiCoP, Ni_2P, and CoP with scanning rates from 20 to 200 mV s^{-1}.

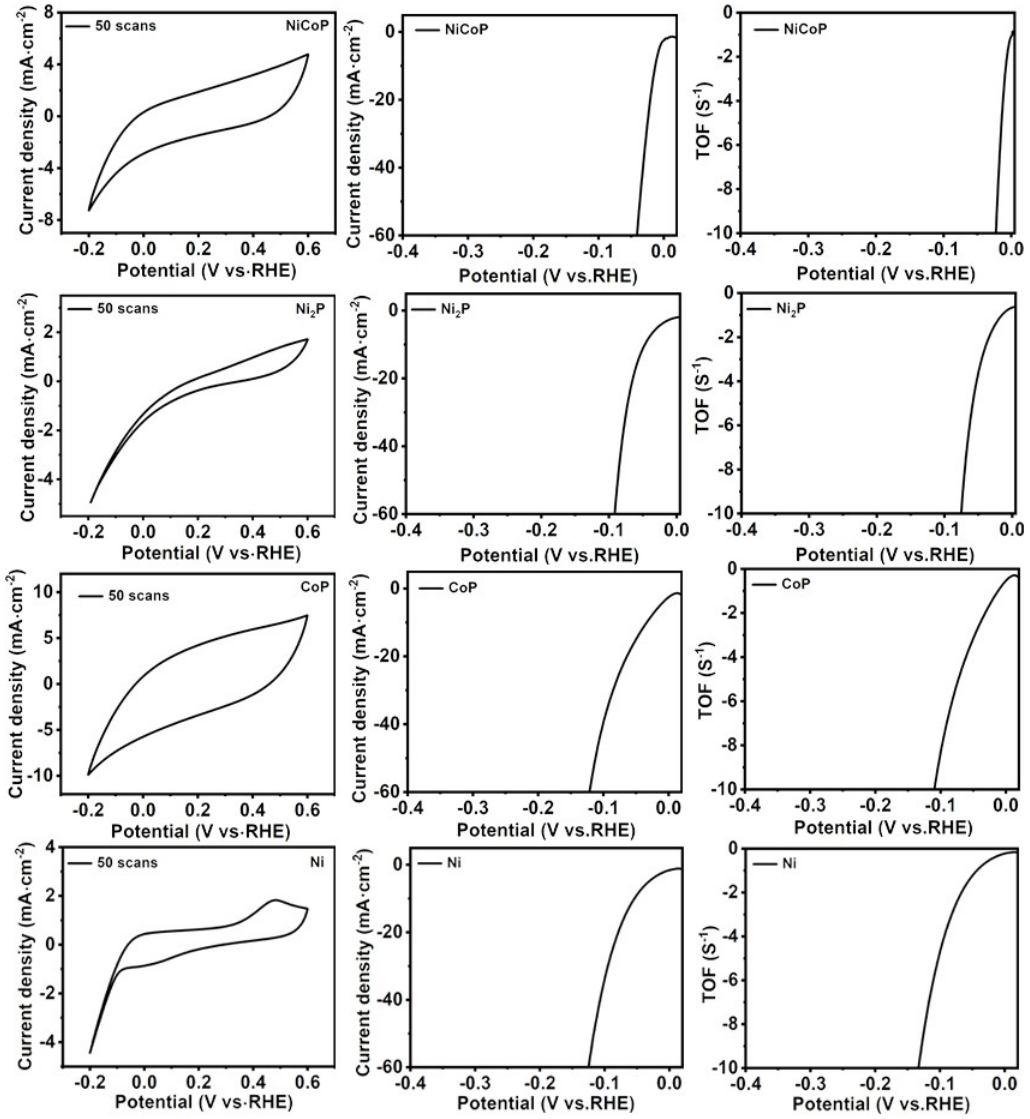

Fig. S12 The cyclic voltammetry curves in the region of − 0.2 to 0.6 V vs. RHE for NiCoP, Ni_2P, CoP, and Ni at pH = 7.0 with a scan rate 50 mV s^{-1}. Polarization curves of NiCoP, Ni_2P, CoP at pH = 1.0 with a scan rate of 5 mV s^{-1}. (c) Calculated TOFs for NiCoP, Ni_2P, CoP at pH = 1.0.

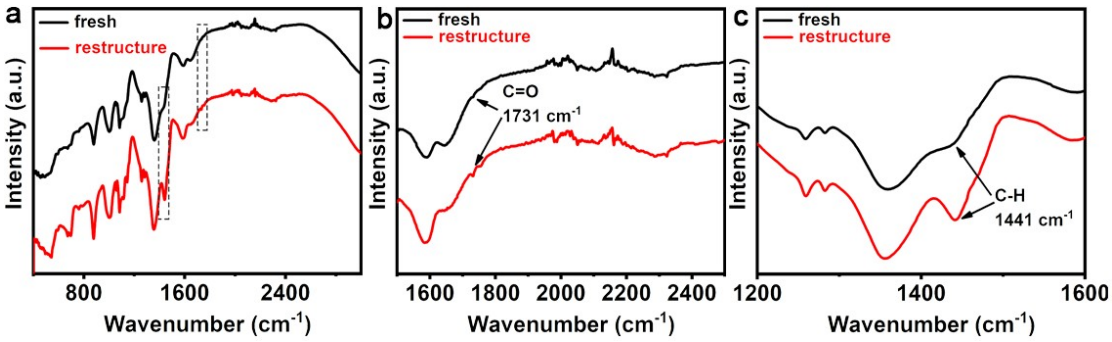

Fig. S13 (a) Adsorption infrared spectra of HMF before and after catalyst reconstruction. (b) and (c) Partial enlargement of infrared spectrum.

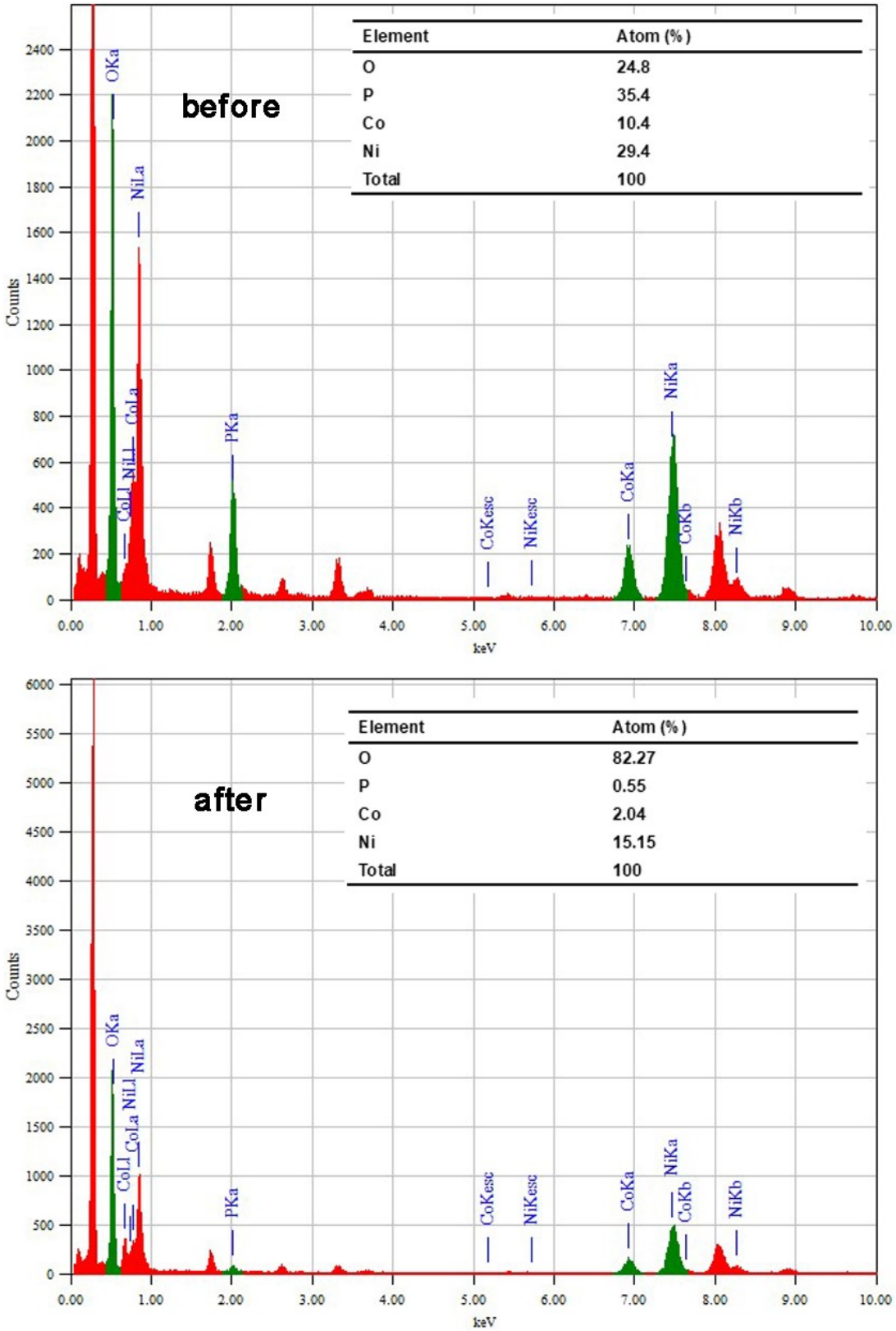

Fig. S14 The EDS elemental content of catalysts before and after HMFOR.

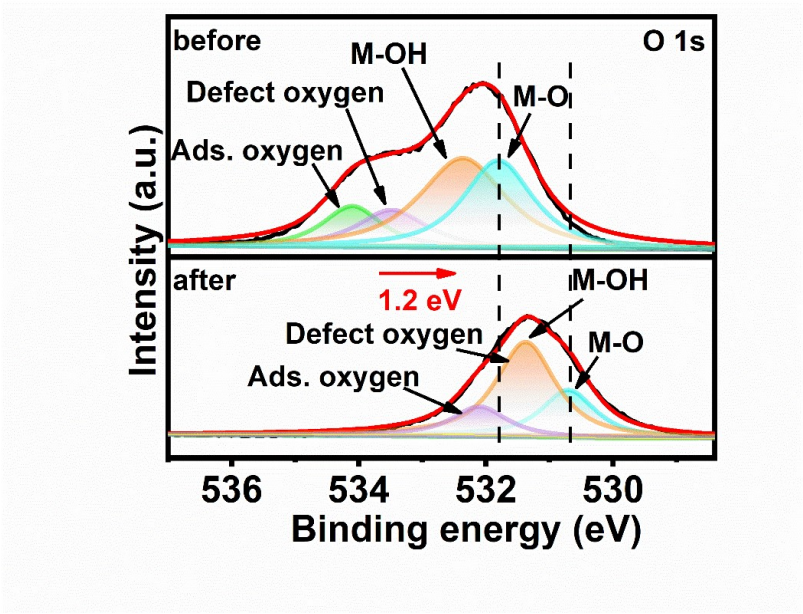

Fig. S15 The XPS spectra of O 1s in the NiCoP before and after HMFOR.

Table S5. The surface element content of NiCoP before and after HMFOR was measured by XPS.

Condition	elements	Atomic (%)
before	C 1s	7.25
	O 1s	58.93
	Co 2p	3.7
	Ni 2p	7.59
	P 2p	22.52
after	C 1s	9.45
	O 1s	59.21
	Co 2p	6.71
	Ni 2p	19
	P 2p	5.63

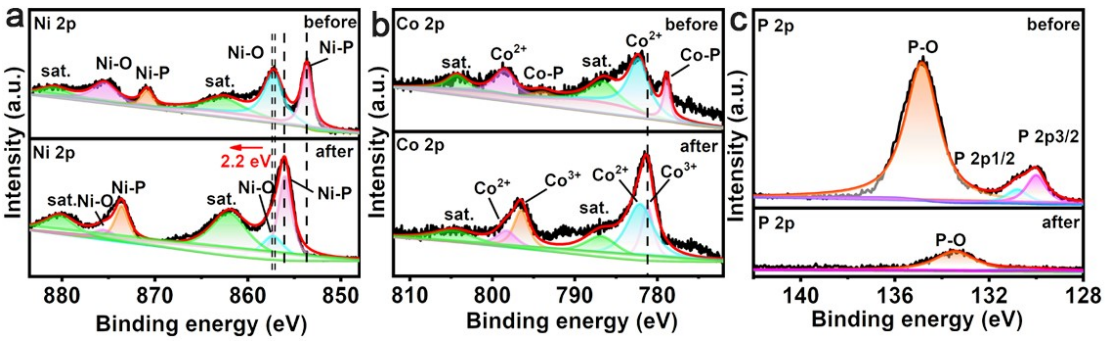

Fig. S16 The XPS analysis of the NiCoP before and after the HMFOR test.

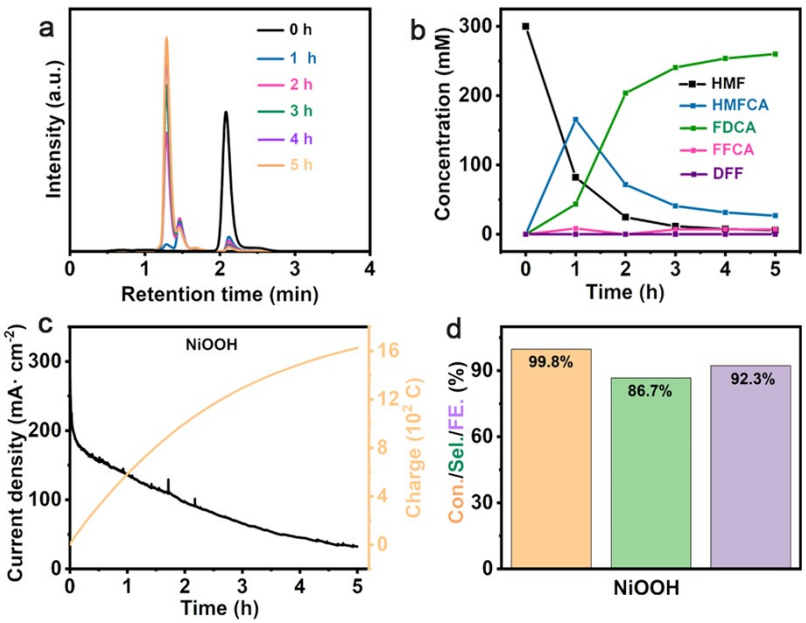

Fig. S17. (a) The chromatogram of HMF electrooxidation catalyzed by NiOOH. (b) Concentration change curves with the progress of reaction for the products during the HMFOR process. (c) I-t curve of NiOOH at a constant potential of 1.464 V via passing the charge of 1627.6 C. (d) HMF conversion, FDCA selectivity, and Faraday efficiency of NiOOH.

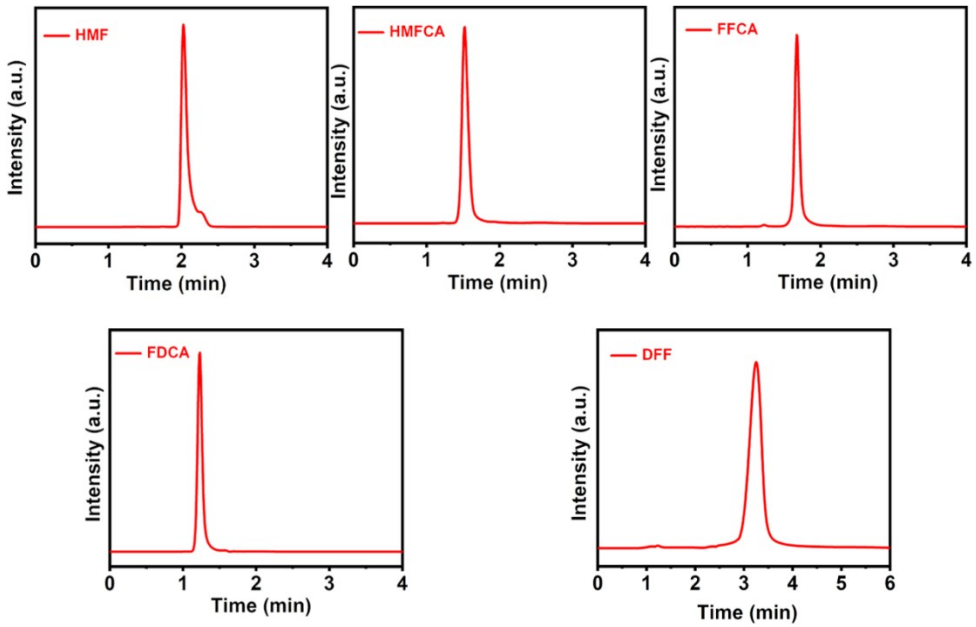

Fig. S18 The HPLC measurements of pure HMF, HMFCA, FFCA, FDCA, and DFF.

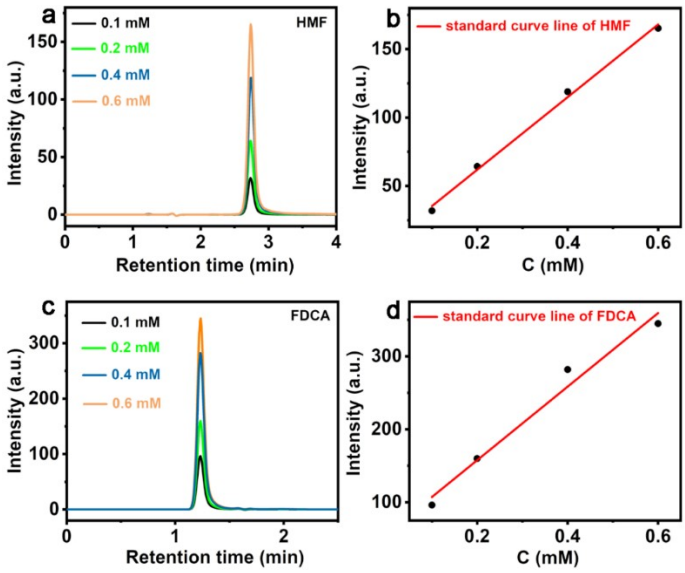

Fig. S19 Calibration curves of the HPLC for HMF and FDCA.

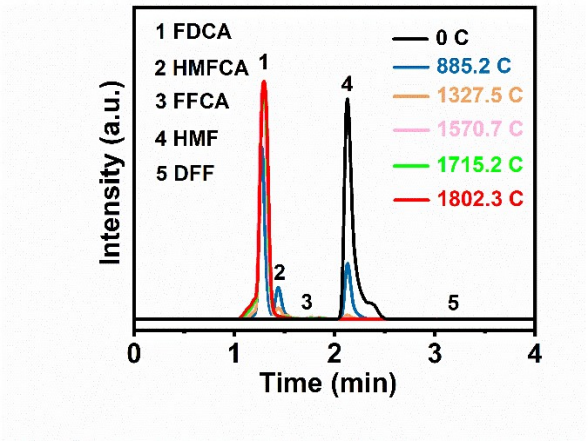

Fig. S20 The chromatogram of HMF electrooxidation catalyzed by NiCoP at 1.464 V in 10 mL 1.0 M KOH with 300 mM HMF.

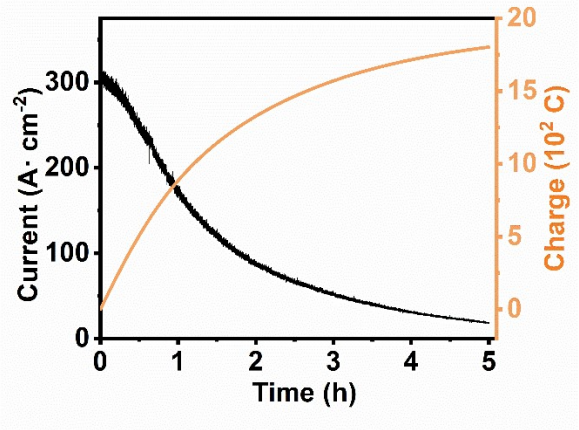

Fig. S21 I-t curve of NiCoP at a constant potential of 1.464 V in 1.0 M KOH with 300 mM HMF via passing the charge of 1802.3 C.

Table S6. The concentration of each substance changed with reaction time.

Substances	Reaction time (h)	Concentration (mM)
HMF	0	300
	1	70.32
	2	4.86
	3	0.99
	4	0.39
	5	0.3
FDCA	0	0
	1	189.13
	2	288.01
	3	298.42
	4	298.83
	5	299.44
HMFCA	0	0
	1	39.59
	2	6.81
	3	0.04
	4	0.39
	5	0.14
FFCA	0	0
	1	0.96
	2	0.32
	3	0.55
	4	0.39
	5	0.12
DFF	0	0
	1	0
	2	0
	3	0
	4	0
	5	0

Table S7. Comparison of conversion, selectivity, and Faraday efficiency for as-prepared samples.

Substances	Conversion rate (%)	Selectivity (%)	Faraday efficiency (%)
NiCoP	99.8	99.6	96.1
Ni_2P	98.8	92.4	90.9
CoP	98	91.3	79.1

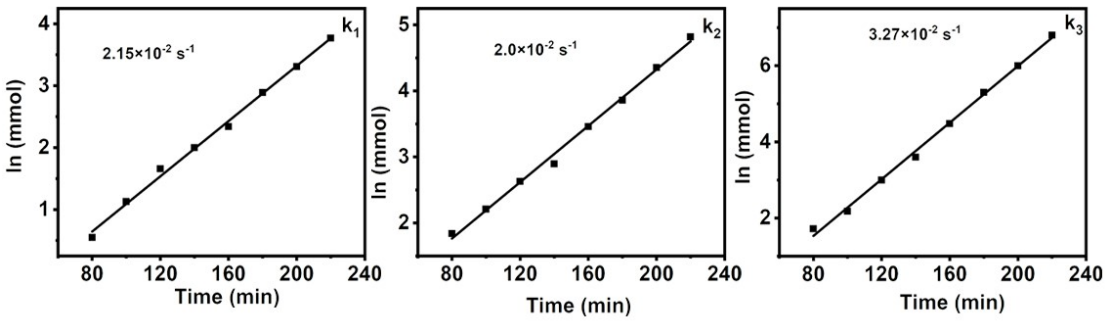

Fig. S22 Estimation of rate constants for each product.

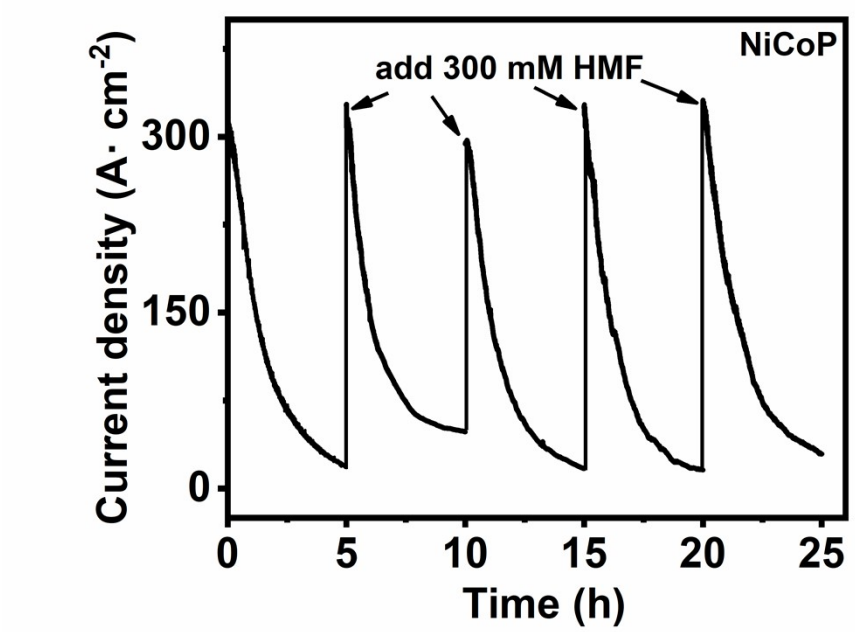

Fig. S23 I-t curve of NiCoP at 1.464 V with the intermittent addition of 300 mM HMF.

Table S8. Various substances analysis five successive cycles HMFOR for NiCoP.

Cycles	Conversion rate (%)	Selectivity (%)	Faraday efficiency (%)
1	99.8	99.2	95.6
2	99.8	99.1	92.9
3	99.8	99.1	95.5
4	99.8	99.1	95.7
5	99.8	99.2	93.5

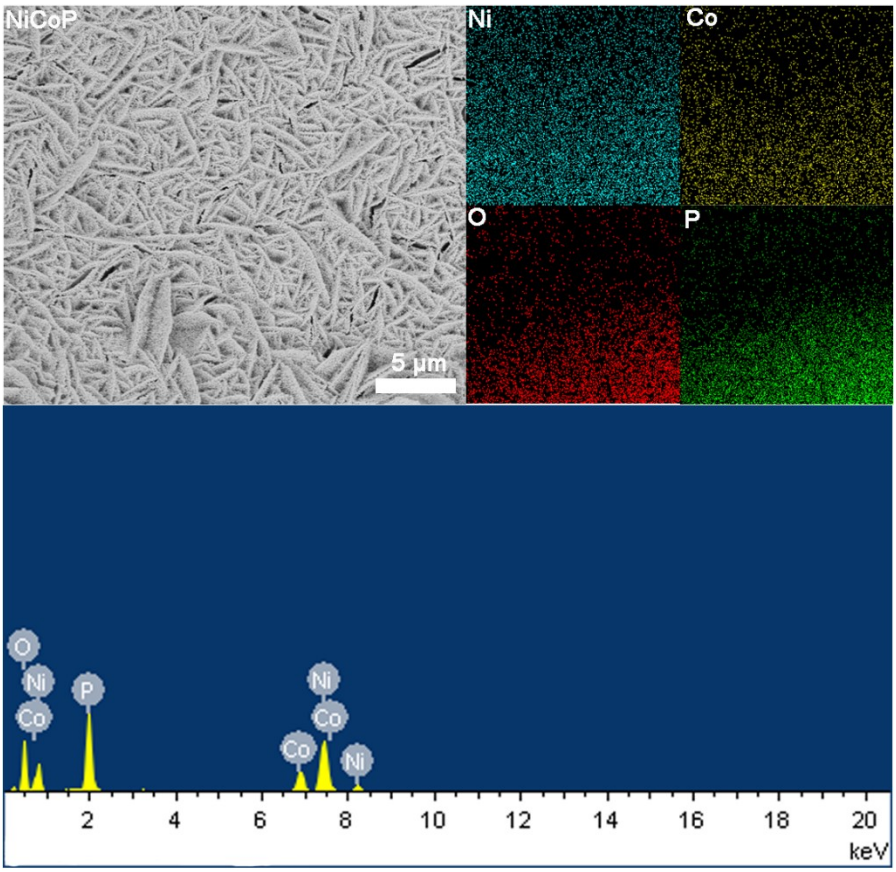

Fig. S24 The SEM image elements mapping and EDS of NiCoP after HMFOR.

Table S9. The mass percentage and atomic percentage of elements in NiCoP catalyst after HMFOR.

Elements	Mass ratio	Atomic
O	24.55	51.86
P	7.13	7.78
Co	16.28	9.34
Ni	52.04	31.02
Total	100	

Table. S10 Conversion, selectivity, and Faraday efficiency of NiCoP coupled flow-through reactor at different flow rates.

Flow rate (mL/min)	Conversion rate (%)	Selectivity (%)	Faraday efficiency (%)
0.05	99.9	98.9	95.4
0.1	99.9	98.6	95.1
0.15	98.7	98.8	94.2
0.2	98.2	90.7	86
0.3	97.3	87.9	82.6
0.4	97	87.1	81.6

Table. S11 Conversion, selectivity, and Faraday efficiency of NiCoP coupled flow-by reactor at different flow rates.

Flow rate (mL/min)	Conversion rate (%)	Selectivity (%)	Faraday efficiency (%)
0.05	99.8	99.7	96.8
0.1	97.7	99	94.1
0.15	96.9	91.7	86.4
0.2	96.4	82.9	82.4
0.3	96.2	86	80.5

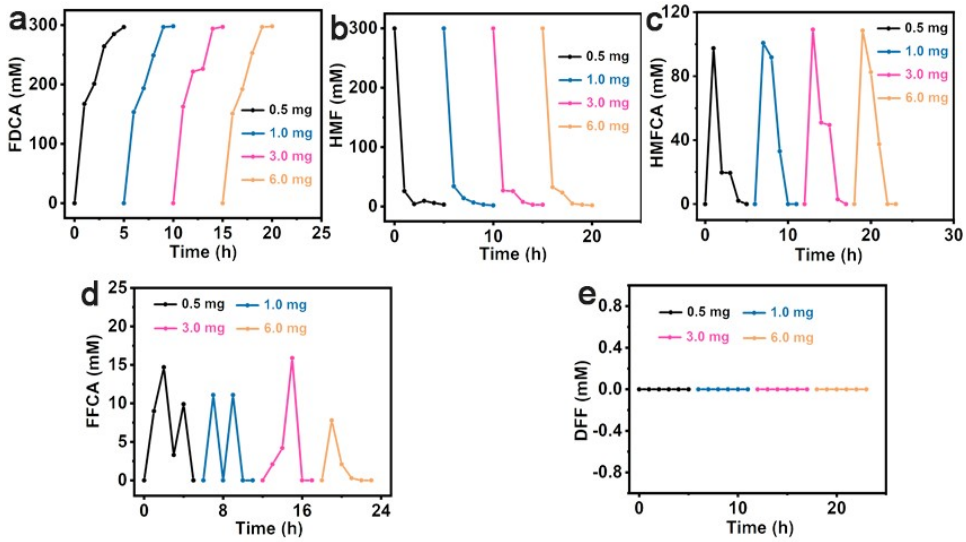

Fig. S25 (a) The effects of different P content in electrolyte on the detection of FDCA, (b) HMF, (c) HMFCA, (d) FFCA and DFF.

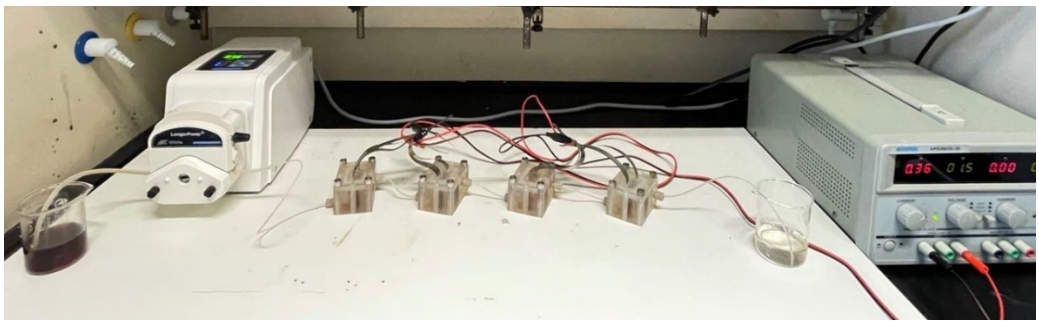

Fig. S26 Evaluation of STY in a flow-through reactor under 1.464 V constant voltage.

Table. S12 Conversion, selectivity, and Faraday efficiency of NiCoP coupled flow- through reactor for ten times.

Cycles	Conversion rate (%)	Selectivity (%)	Faraday efficiency (%)
1	99.9	98.9	94.2
2	99.9	98.9	94.2
3	99.9	97.8	93.1
4	99.9	97.3	93
5	99.9	97.3	92.6
6	99.9	97.4	92.6
7	99.9	97	92.4
8	99.9	97	92.4
9	99.9	97	92.4
10	99.9	97	92.4

Notes and references

1 B. J. Taitt, D. H. Nam, K. S. Choi, *ACS Catal*., 2018, **9**, 660-670.

2 G. Yang, Y. Jiao, H. Yan, Y. Xie, A. Wu, X. Dong, D. Guo, C. Tian, H. Fu, *Adv. Mater.*, 2020, **32**, 2000455.

3 L. Gao, Z. Liu, J. Ma, L. Zhong, Z. Song, J. Xu, S. Gan, D. Han, L. Niu, *Appl. Catal. B-Environ*., 2020, **261**, 118235.

4 N. Zhang, Y. Zou, L. Tao, W. Chen, L. Zhou, Z. Liu, B. Zhou, G. Huang, H. Lin, S. Wang, *Angew. Chem., Int. Ed*., 2019, **58**, 15895-15903.

5 N. Jiang, B. You, R. Boonstra, I. M. Terrero Rodriguez, Y. Sun, *ACS Energy Lett*, 2016, **1**, 386-390.

6 M. J. Kang, H. Park, J. Jegal, S. Y. Hwang, Y. S. Kang, H. G. Cha, Appl. Catal. B-Environ., 2019, **242**, 85-91.

7 S. Li, X. Sun, Z. Yao, X. Zhong, Y. Cao, Y. Liang, Z. Wei, S. Deng, G. Zhuang, X. Li, J. Wang, *Adv. Funct. Mater.*, 2019, **29**, 1904780.

8 Y. Peng, W. Pan, N. Wang, J. E. Lu, S. Chen, ChemSusChem., 2018, **11**, 130-136.

9 Y. Lu, C. L. Dong, Y. C. Huang, Y. Zou, Z. Liu, Y. Liu, Y. Li, N. He, J. Shi, S. Wang, *Angew. Chem., Int. Ed*., 2020, **59**, 19215-19221.

10 M. Zhang, Y. Liu, B. Liu, Z. Chen, H. Xu, K. Yan, *ACS Catal*, 2020,**10**, 5179-5189.

11 I. van Scodeller, K. De Oliveira Vigier, E. Muller, C. Ma, F. Guegan, R. Wischert, F. Jerome, ChemSusChem, 2021, **14**, 313-323.

12 M. Park, M. Gu, B. S. Kim, *ACS Nano*, 2020, **14**, 6812-6822.

13 W. Zhong, B. Xiao, Z. Lin, Z. Wang, L. Huang, S. Shen, Q. Zhang, L. Gu, *Adv. Mater.*, 2021, **33**, 2007894.

14 J. Song, Y. Q. Jin, L. Zhang, P. Dong, J. Li, F. Xie, H. Zhang, J. Chen, Y. Jin, H. Meng, X. Sun, *Adv. Energy Mater.*, 2021, **11**, 2003511.

15 Q. Qian, J. Zhang, J. Li, Y. Li, X. Jin, Y. Zhu, Y. Liu, Z. Li, A. El-Harairy, C. Xiao, G. Zhang, Y. Xie, *Angew. Chem., Int. Ed.*, 2021, **60**, 5984-5993.

16 W. Du, Y. Shi, W. Zhou, Y. Yu, B. Zhang, *Angew. Chem., Int. Ed.*, 2021, **60**, 7051-7055.

17 Y. Gu, A. Wu, Y. Jiao, H. Zheng, X. Wang, Y. Xie, L. Wang, C. Tian, H. Fu, *Angew. Chem., Int. Ed.*, 2021, **60**, 6673-6681.

18 Q. Fu, X. Wang, J. Han, J. Zhong, T. Zhang, T. Yao, C. Xu, T. Gao, S. Xi, C. Liang, L. Xu, P. Xu, B. Song, *Angew. Chem., Int. Ed.*, 2021, **60**, 259-267.

19 J. Kim, H. Jung, S. M. Jung, J. Hwang, D. Y. Kim, N. Lee, K. S. Kim, H. Kwon, Y. T. Kim, J. W. Han, J. K. Kim, *J. Am. Chem. Soc.*, 2021, **143**, 1399-1408.

20 L. Yu, J. Zhang, Y. Dang, J. He, Z. Tobin, P. Kerns, Y. Dou, Y. Jiang, Y. He, S. L. Suib, *ACS Catal*, 2019, **9**, 6919-6928.

21 C. Zhang, X. Liang, R. Xu, C. Dai, B. Wu, G. Yu, B. Chen, X. Wang, N. Liu, *Adv. Funct. Mater.*, 2021, **31**, 2008298.

22 R. Q. Yao, Y. T. Zhou, H. Shi, W. B. Wan, Q. H. Zhang, L. Gu, Y. F. Zhu, Z. Wen, X. Y. Lang, Q. Jiang, *Adv. Funct. Mater.*, 2020, **31**, 2009613.

23 P. Sabhapathy, I. Shown, A. Sabbah, P. Raghunath, J. L. Chen, W. F. Chen, M. C. Lin, K. H. Chen, L. C. Chen, *Nano Energy*, 2021, **80**, 105544.

24 G. Meng, H. Tian, L. Peng, Z. Ma, Y. Chen, C. Chen, Z. Chang, X. Cui, J. Shi, *Nano Energy*, 2021, **80**, 105531.

25 X. Huang, H. Xu, D. Cao, D. Cheng, *Nano Energy*, 2020, **78**, 105253.

26 L. Zhao, H. Yuan, D. Sun, J. Jia, J. Yu, X. Zhang, X. Liu, H. Liu, W. Zhou, *Nano Energy*, 2020, **77**, 105056.

27 P. Zhou, G. Zhai, X. Lv, Y. Liu, Z. Wang, P. Wang, Z. Zheng, H. Cheng, Y. Dai, B. Huang, *Appl. Catal. B-Environ*., 2021, **283**, 119590.

28 C. Huang, L. Yu, W. Zhang, Q. Xiao, J. Zhou, Y. Zhang, P. An, J. Zhang, Y. Yu, *Appl. Catal. B-Environ*., 2020, **276**, 119137.

29 K. Tu, D. Tranca, F. Rodriguez-Hernandez, K. Jiang, S. Huang, Q. Zheng, M.X. Chen, C. Lu, Y. Su, Z. Chen, H. Mao, C. Yang, J. Jiang, H. W. Liang, X. Zhuang, *Adv. Mater*., 2020, **32**, 2005433.

30 I. S. Kwon, I. H. Kwak, S. Ju, S. Kang, S. Han, Y. C. Park, J. Park, J. Park, *ACS Nano*, 2020,**14**, 12184-12194.